

Supporting Information

Single crystal field-effect transistors of a highly dipolar merocyanine dye

Andreas Liess, Matthias Stolte, Tao He and Frank Würthner*

Universität Würzburg, Institut für Organische Chemie & Center for Nanosystems Chemistry,
Am Hubland, 97074 Würzburg, Germany.

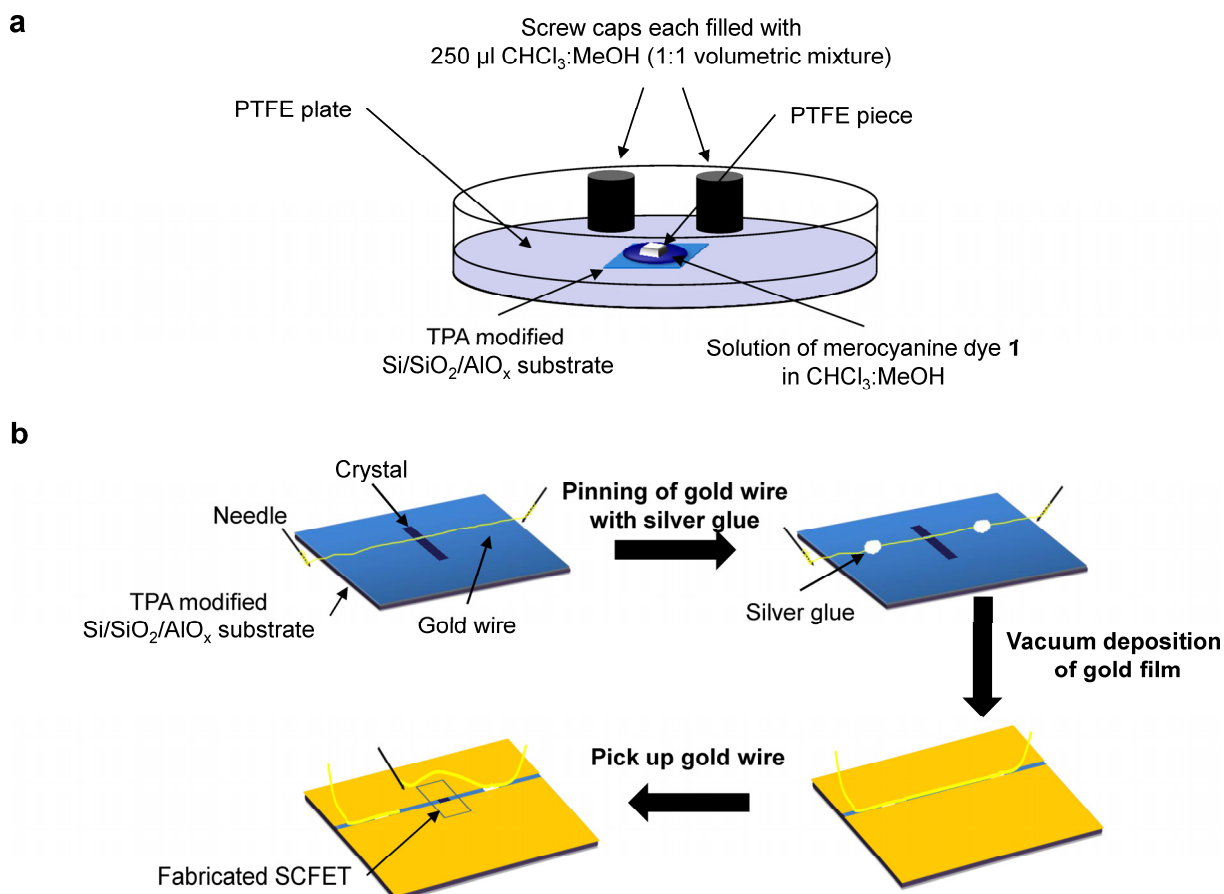


Fig. S1. (a) Schematic drawing of crystal growth procedure on TPA modified $\text{Si/SiO}_2/\text{AlO}_x$ substrate. (b) Schematic drawing of fabrication of gold source and drain electrodes onto a grown single crystal.

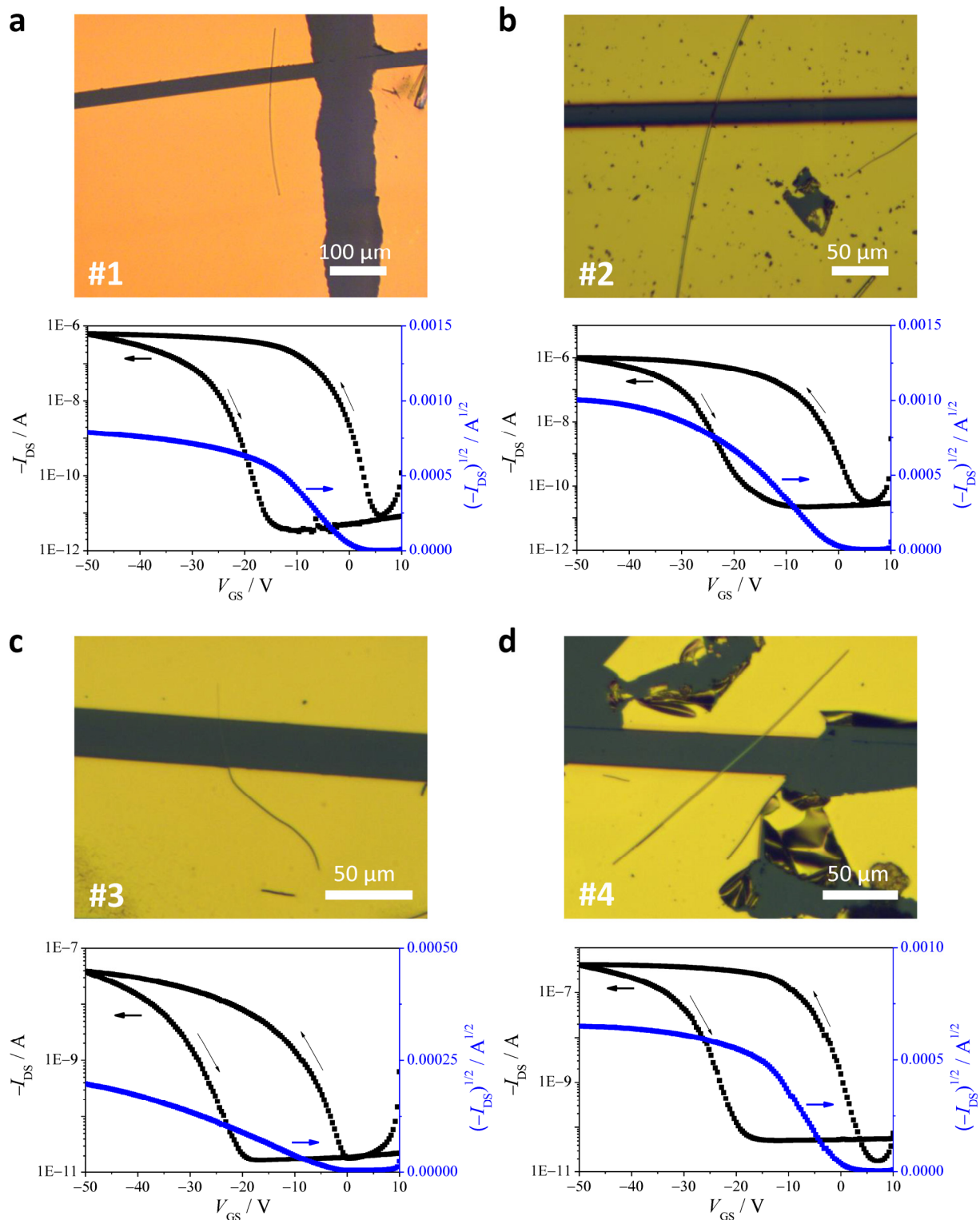


Fig. S2. Optical microscopy images and corresponding transfer characteristics of SCFET devices #1 (a), #2 (b), #3 (c) and #4 (d).

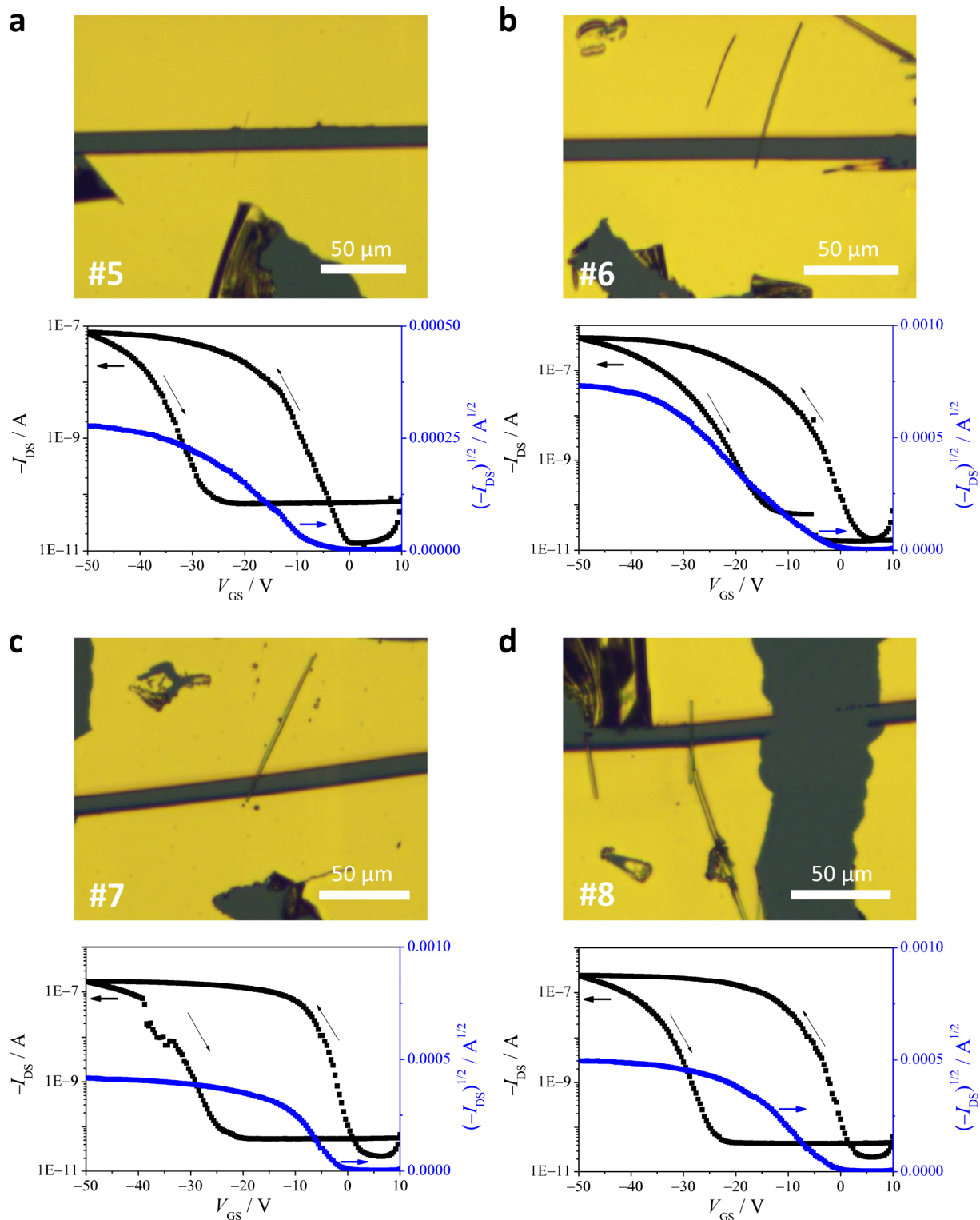


Fig. S3. Optical microscopy images and corresponding transfer characteristics of SCFET devices #5 (a), #6 (b), #7 (c) and #8 (d).

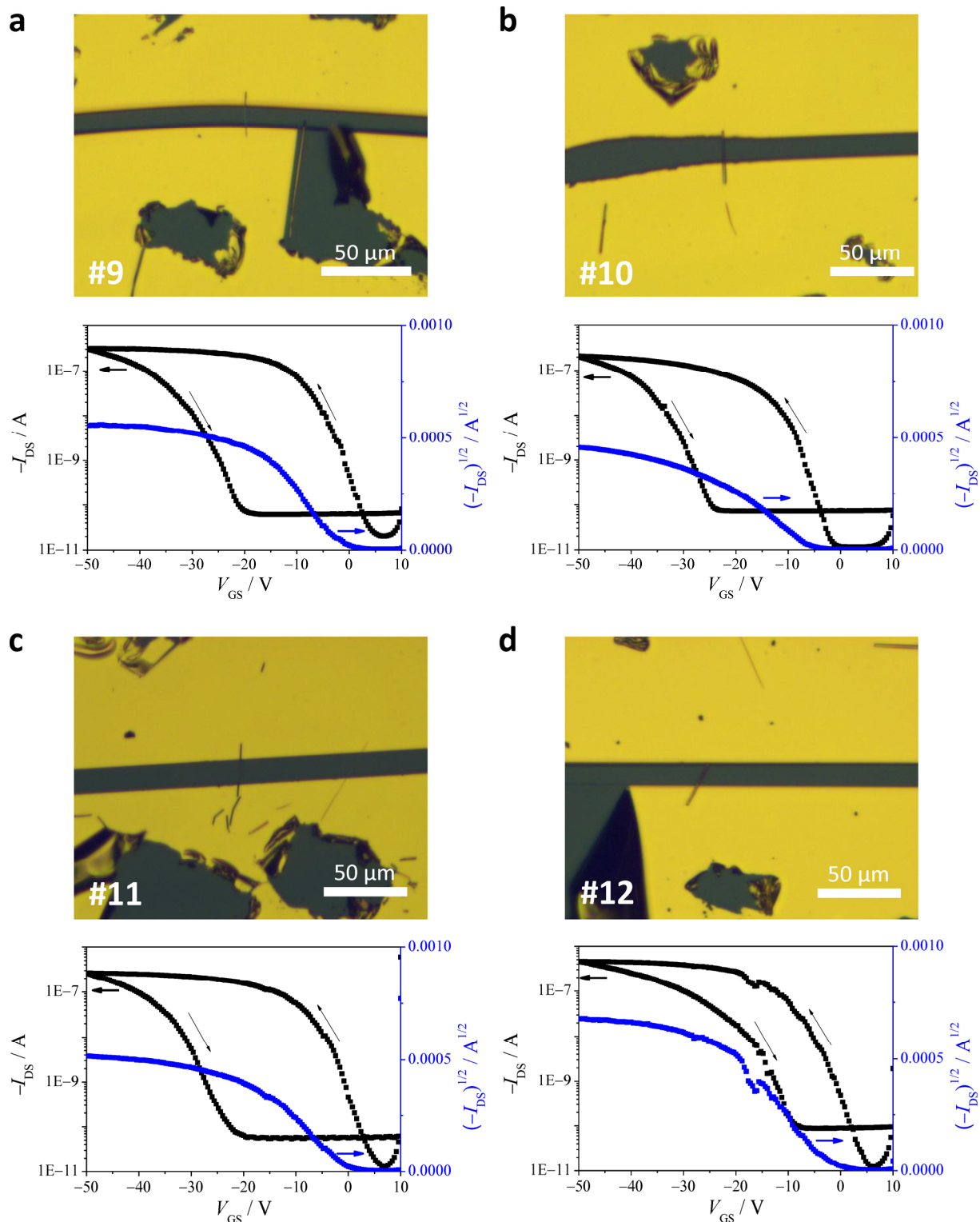


Fig. S4. Optical microscopy images and corresponding transfer characteristics of SCFET devices #9 (a), #10 (b), #11 (c) and #12 (d).

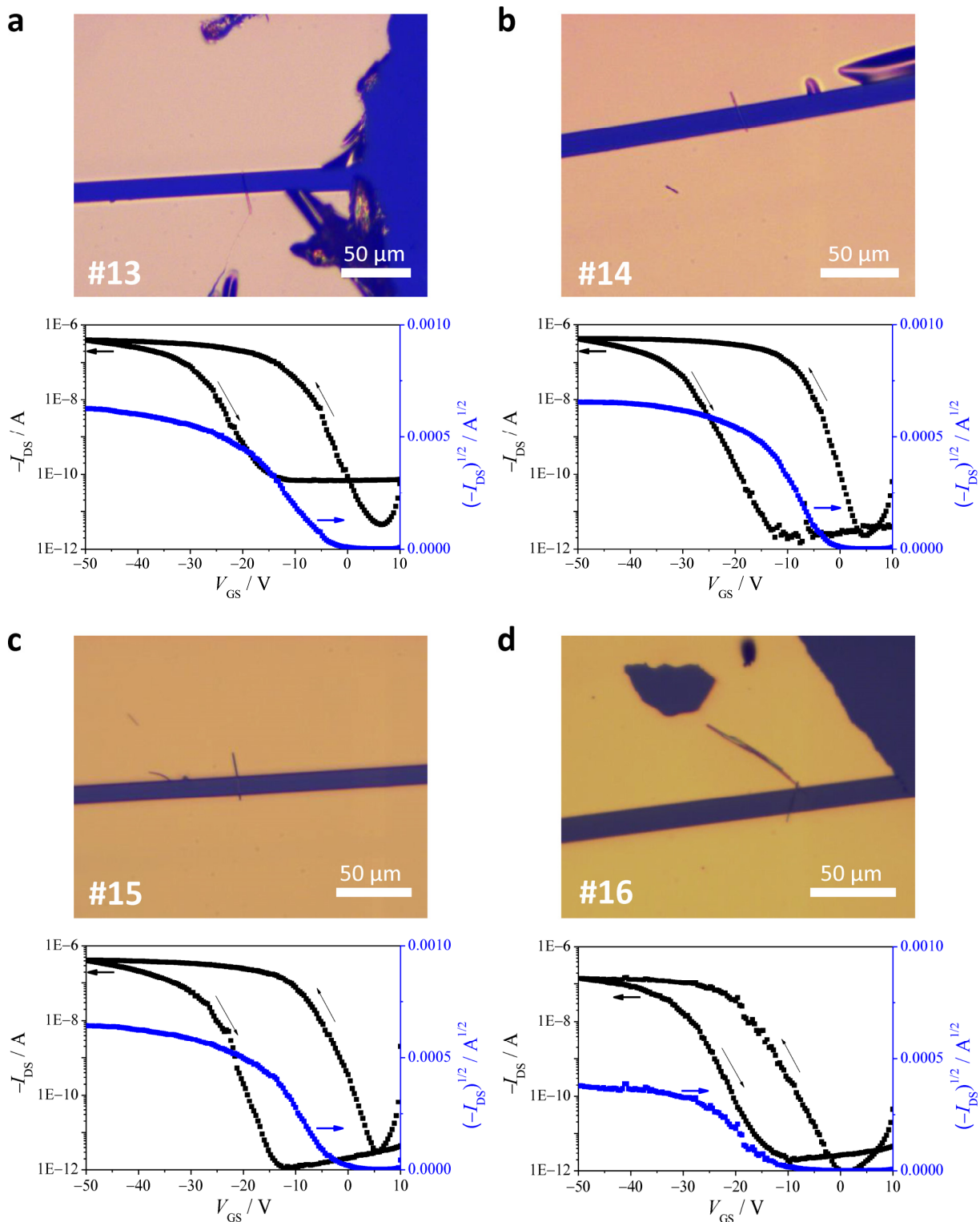


Fig. S5. Optical microscopy images and corresponding transfer characteristics of SCFET devices #13 (a), #14 (b), #15 (c) and #16 (d).

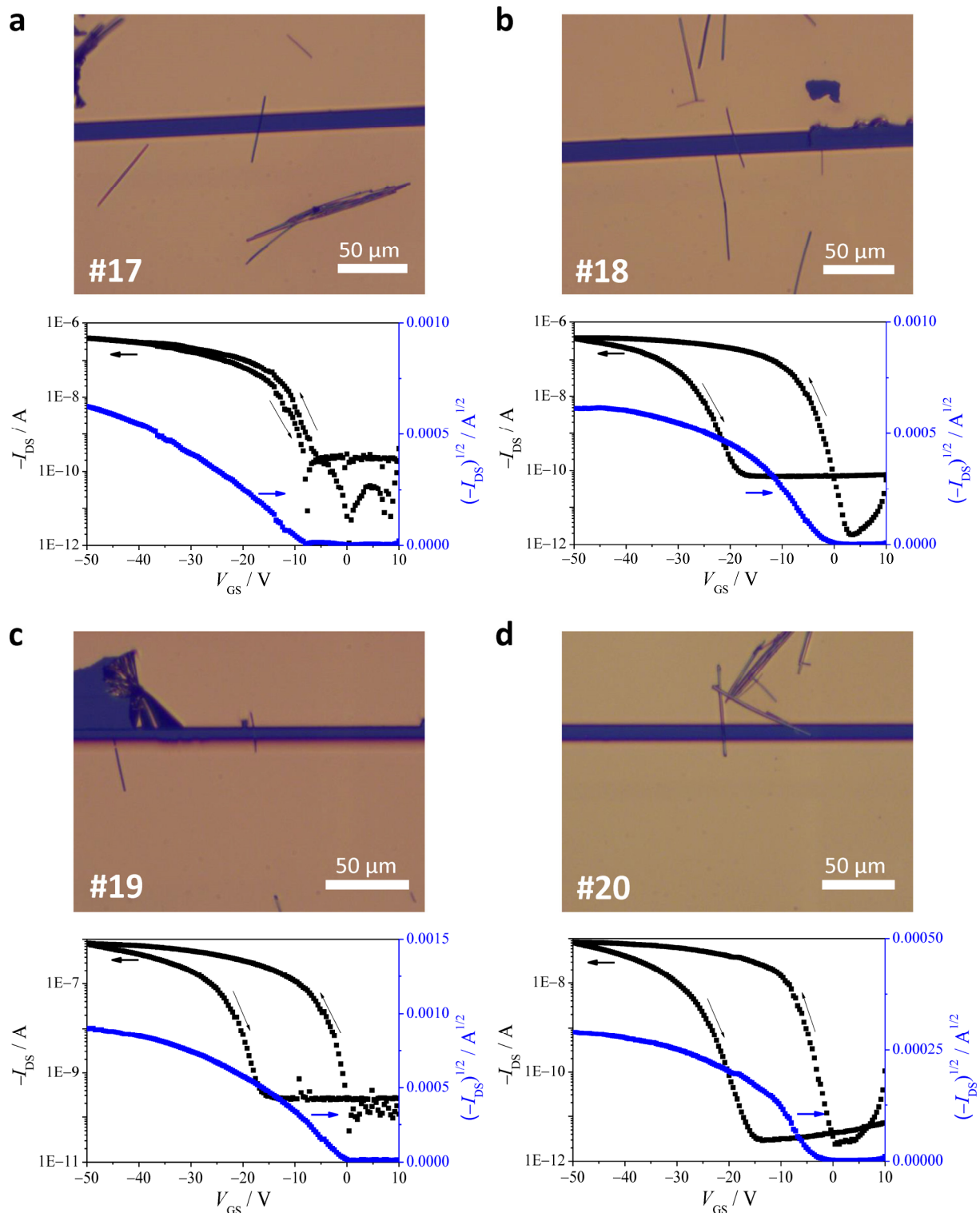


Fig. S6. Optical microscopy images and corresponding transfer characteristics of SCFET devices #17 (a), #18 (b), #19 (c) and #20 (d).

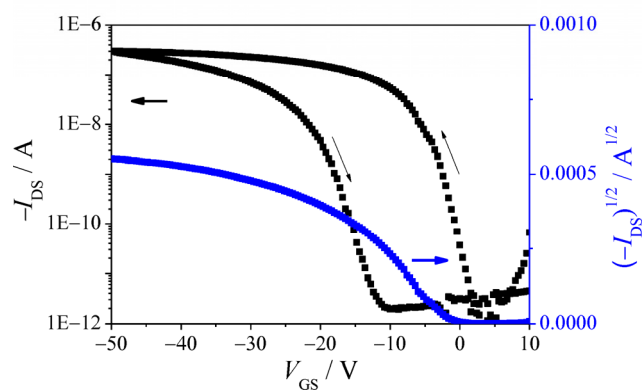
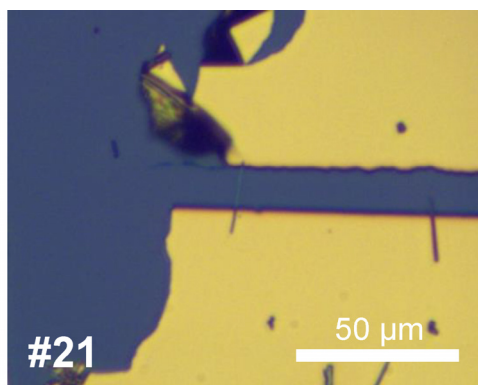


Fig. S7. Optical microscopy image and corresponding transfer characteristic of SCFET device #21.

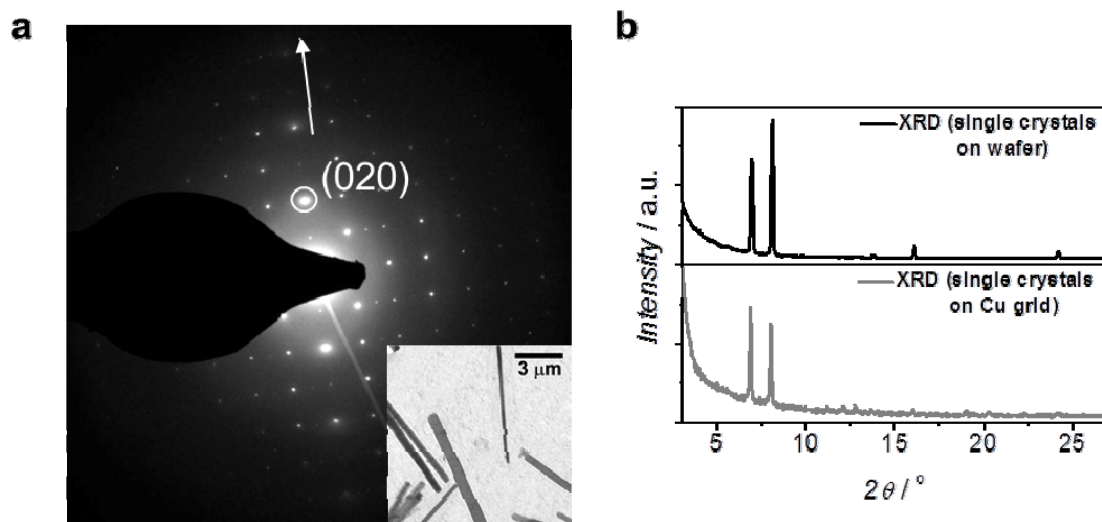


Fig. S8. (a) SAED pattern of a single crystal of merocyanine dye **1** with indicated direction of crystal elongation as white arrow (inset: transmission electron microscopy image of single crystals of dye **1** used for SAED experiments). (b) XRD pattern of single crystals of merocyanine dye **1** on a copper grid used for SAED measurements in comparison to the XRD pattern of the single crystals of merocyanine dye **1** on the TPA modified Si/SiO₂/AlO_x substrate.

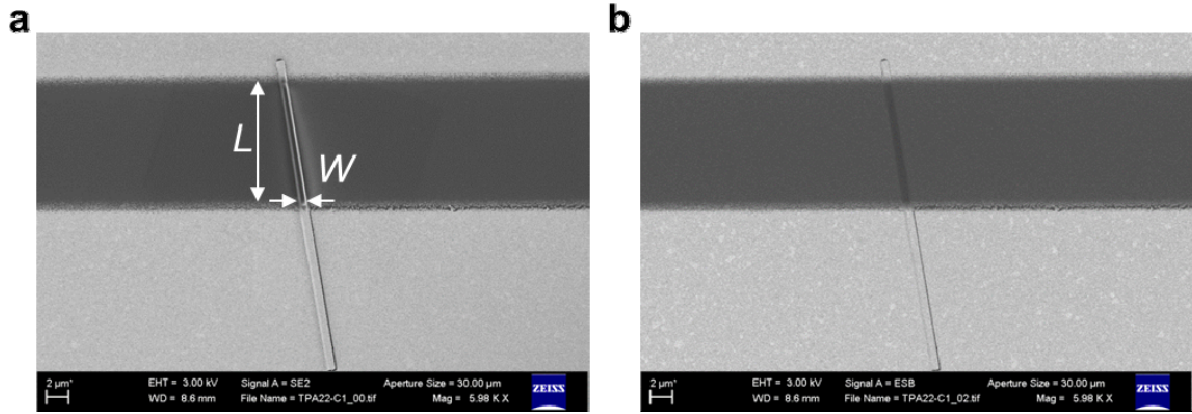


Fig. S9. SEM images of representative device obtained with secondary electron detector (a) and backscattered electron detector (b) for conservative determination of the device dimensions as indicated in (a).

Tab. S1. Channel length (L), channel width (W), crystal thickness (d), charge carrier mobility (μ), threshold voltage (V_T) and current on/off ratio (I_{on}/I_{off}) of all fabricated SCFETs of merocyanine dye **1**.

#	L / μm	W / μm	d / nm	μ / $\text{cm}^2 \text{V}^{-1} \text{s}^{-1}$	V_T / V	I_{on}/I_{off}
1	23.4	1.7	195	1.38	0	$2 \cdot 10^5$
2	12.4	2.0	170	0.56	-1	$5 \cdot 10^4$
3	25.1	0.2	49	0.22	-3	$2 \cdot 10^3$
4	23.2	1.9	75	1.03	0	$2 \cdot 10^4$
5	10.5	0.2	64	0.42	-6	$6 \cdot 10^3$
6	9.6	1.0	145	0.37	-6	$3 \cdot 10^4$
7	9.6	1.6	930	0.33	-1	$8 \cdot 10^3$
8	7.4	1.1	658	0.26	-2	$1 \cdot 10^4$
9	9.0	0.4	103	1.45	-2	$2 \cdot 10^4$
10	12.9	1.1	730	0.26	-5	$2 \cdot 10^4$
11	13.4	0.6	169	0.84	0	$5 \cdot 10^4$
12	11.1	1.7	742	0.41	-3	$4 \cdot 10^4$
13	11.0	0.8	394	0.82	-4	$9 \cdot 10^4$
14	13.0	1.0	313	1.47	-3	$3 \cdot 10^5$
15	10.5	0.4	128	2.34	-3	$4 \cdot 10^5$
16	12.0	0.6	319	0.83	-13	$2 \cdot 10^5$
17	10.2	0.5	203	0.69	-9	$1 \cdot 10^4$
18	11.2	0.4	104	1.74	-2	$2 \cdot 10^5$
19	3.8	0.3	87	0.95	0	$2 \cdot 10^4$
20	8.1	1.4	637	0.11	-3	$3 \cdot 10^4$
21	10.3	0.3	77	1.72	-2	$3 \cdot 10^5$
22	11.9	1.1	818	no field effect		

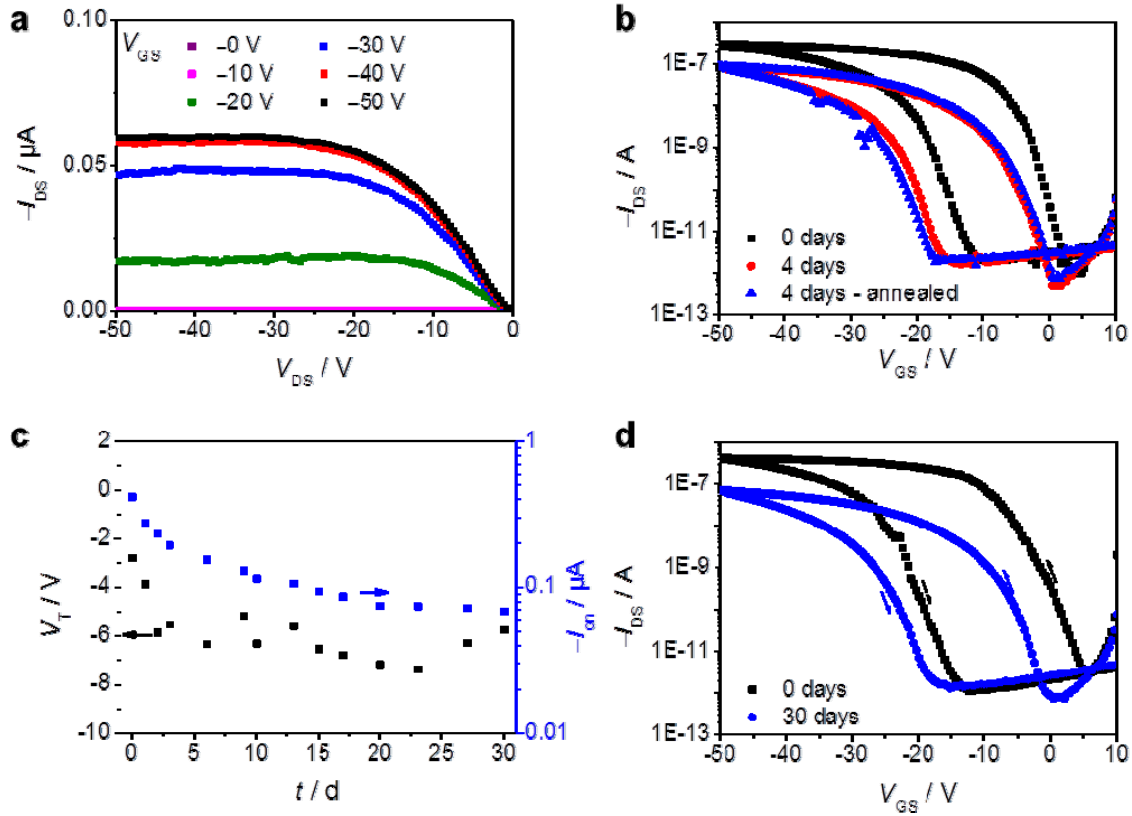


Fig. S10. (a) Output curve of device #15. (b) Transfer characteristics of device #21 as measured after fabrication (0 days), after 4 days in air as well as after 4 days in air and vacuum annealing for 2 h at 100 °C. (c) Development of threshold voltage and on-current of device #15 over 30 days in air. (d) Transfer characteristics of device #15 as measured directly after fabrication and after keeping the device for 30 days in air.

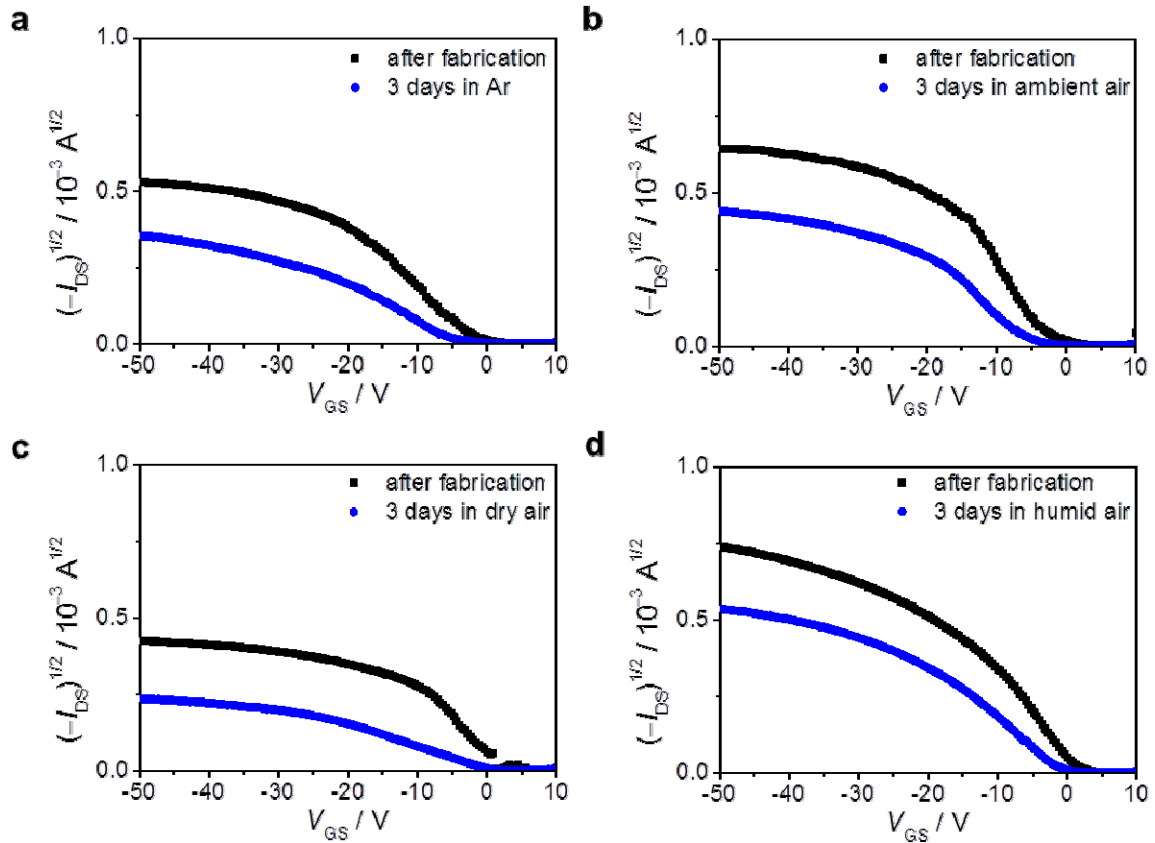


Fig. S11. Square root of the drain-source current of different devices after fabrication as well as after storage for 3 days in Argon (a), ambient air (b), dry air (c) as well as air with 100 % relative humidity (d).

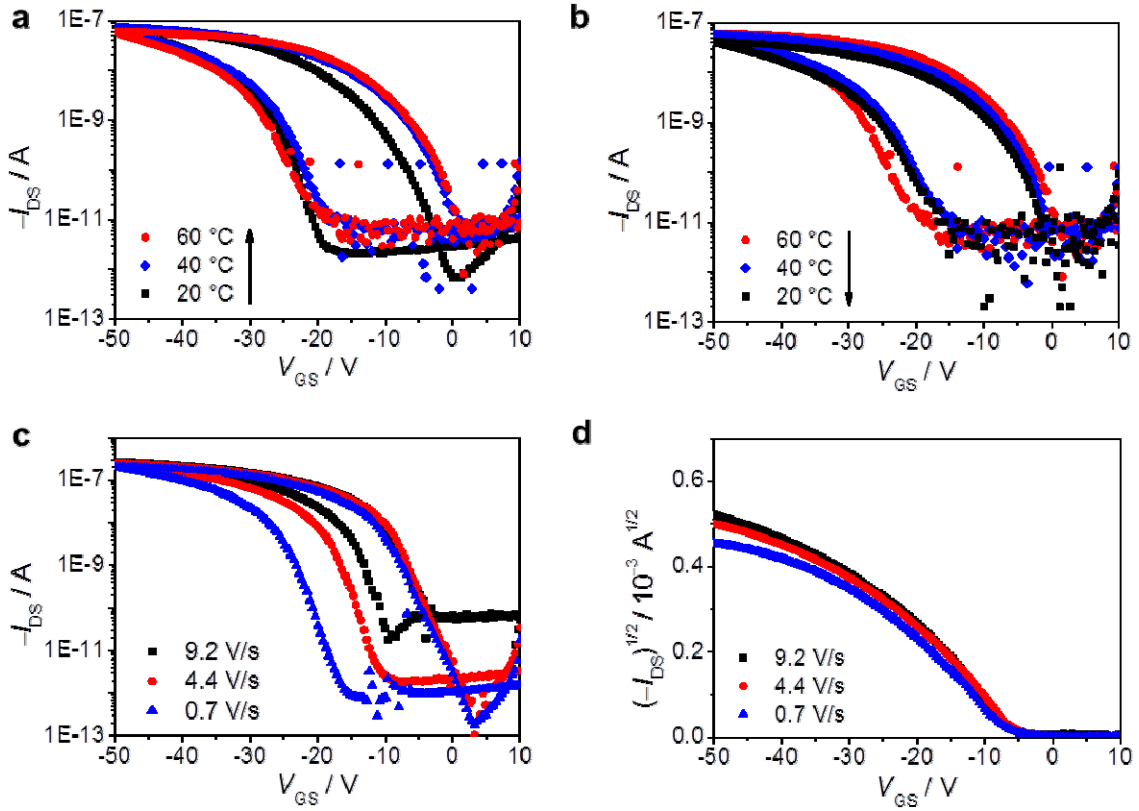


Fig. S12. (a) Transfer characteristics of device #21 measured at different device temperatures upon heating of the device. (b) Transfer characteristics of device #21 measured at different device temperatures upon cooling of the device. (c) Transfer characteristics of device #21 for different sweep rates. (d) Corresponding plot of the square root of the drain-source current of device #21 for different sweep rates.

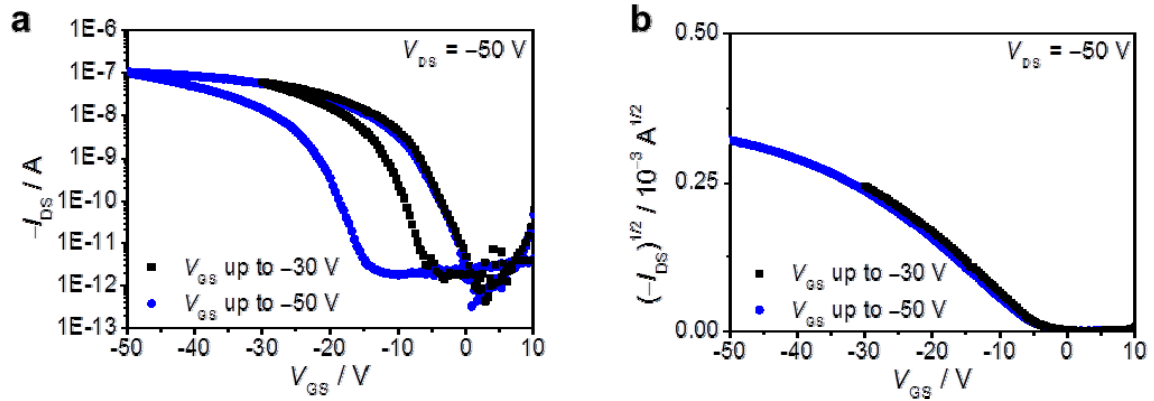


Fig. S13. Transfer characteristics (a) as well as corresponding plot of the square root of the drain-source current (b) of representative device measured at a drain-source voltage of $V_{DS} = -50$ V from $V_{GS} = 10$ V up to $V_{GS} = -30$ V (black squares) and $V_{GS} = -50$ V (blue circles).

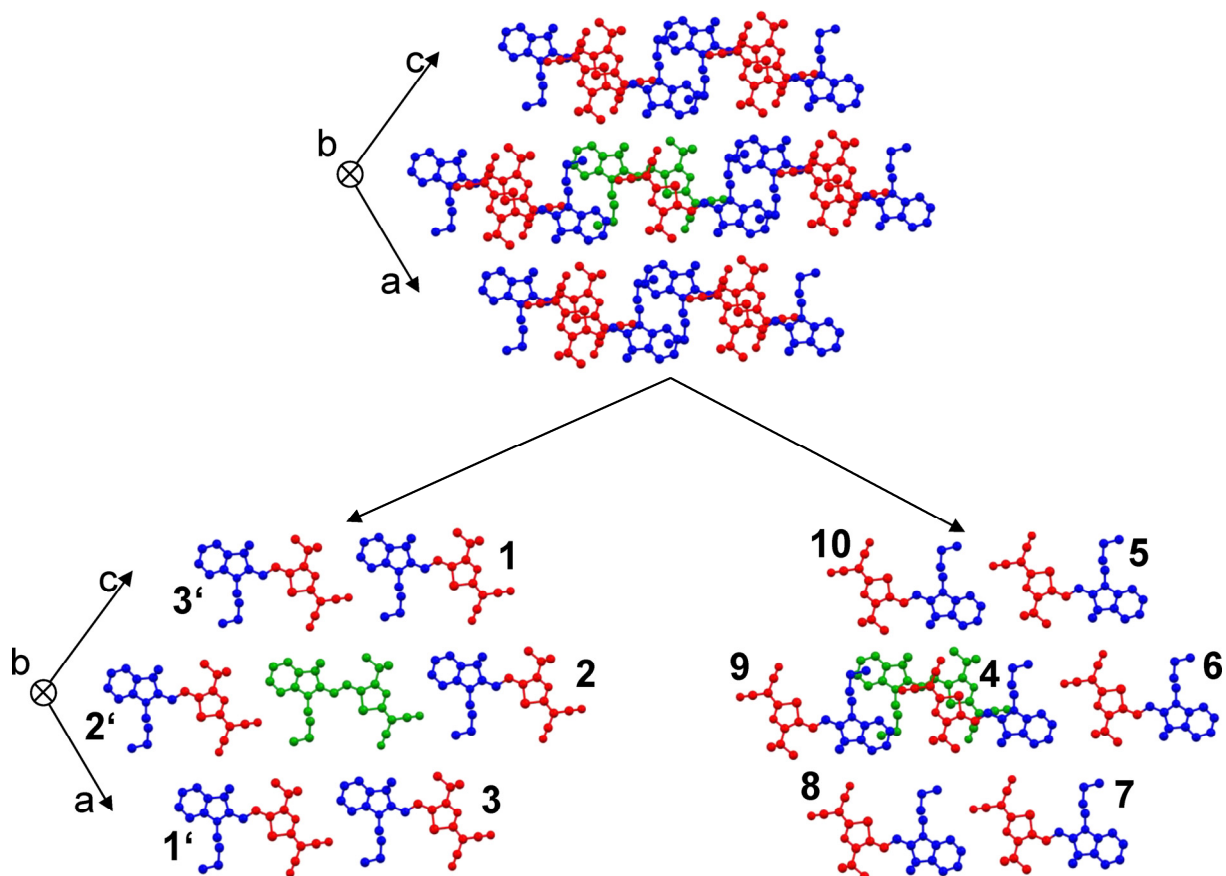


Fig. S14. Numeration of the next neighboring molecules around the central molecule (colored in green). The transfer integrals were calculated for the molecular pairs of the central molecule with a numbered molecule.

Tab. S2. Calculated transfer integrals t of central molecule with next neighboring molecule.

Next neighboring molecule	$ t $ / meV
1/1'	0
2/2'	8
3/3'	9
4	15
5	0
6	0
7	0
8	0
9	0
10	0